Single-Channel Properties of Inositol (1,4,5)-Trisphosphate Receptor Heterologously Expressed in HEK-293 Cells

Elena Kaznacheyeva, Vitalie D. Lupu, and Ilya Bezprozvanny

From the Department of Physiology, University of Texas Southwestern Medical Center at Dallas, Dallas, Texas 75235-9040

ABSTRACT The inositol (1,4,5)-trisphosphate receptor ($InsP_3R$) mediates Ca^{2+} release from intracellular stores in response to generation of second messenger $InsP_3$. $InsP_3R$ was biochemically purified and cloned, and functional properties of native $InsP_3$-gated Ca^{2+} channels were extensively studied. However, further studies of $InsP_3R$ are obstructed by the lack of a convenient functional assay of expressed $InsP_3R$ activity. To establish a functional assay of recombinant $InsP_3R$ activity, transient heterologous expression of neuronal rat $InsP_3R$ cDNA ($InsP_3R$-I, SI− SII+ splice variant) in HEK-293 cells was combined with the planar lipid bilayer reconstitution experiments. Recombinant $InsP_3R$ retained specific $InsP_3$ binding properties (K_d = 60 nM $InsP_3$) and were specifically recognized by anti–$InsP_3R$-I rabbit polyclonal antibody. Density of expressed $InsP_3R$-I was at least 20-fold above endogenous $InsP_3R$ background and only 2–3-fold lower than $InsP_3R$ density in rat cerebellar microsomes. When incorporated into planar lipid bilayers, the recombinant $InsP_3R$ formed a functional $InsP_3$-gated Ca^{2+} channel with 80 pS conductance using 50 mM Ba^{2+} as a current carrier. Mean open time of recombinant $InsP_3$-gated channels was 3.0 ms; closed dwell time distribution was double exponential and characterized by short (18 ms) and long (130 ms) time constants. Overall, gating and conductance properties of recombinant neuronal rat $InsP_3R$-I were very similar to properties of native rat cerebellar $InsP_3R$ recorded in identical experimental conditions. Recombinant $InsP_3R$ also retained bell-shaped dependence on cytosolic Ca^{2+} concentration and allosteric modulation by ATP, similar to native cerebellar $InsP_3R$. The following conclusions are drawn from these results. (*a*) Rat neuronal $InsP_3R$-I cDNA encodes a protein that is either sufficient to produce $InsP_3$-gated channel with functional properties identical to the properties of native rat cerebellar $InsP_3R$, or it is able to form a functional $InsP_3$-gated channel by forming a complex with proteins endogenously expressed in HEK-293 cells. (*b*) Successful functional expression of $InsP_3R$ in a heterologous expression system provides an opportunity for future detailed structure–function characterization of this vital protein.

KEY WORDS: calcium channel • ryanodine receptor • planar lipid bilayer • calcium signaling

INTRODUCTION

Release of Ca^{2+} from intracellular stores in response to generation of the second messenger inositol (1,4,5)-trisphosphate ($InsP_3$)[1] is a common mechanism used by many cell types to raise cytosolic Ca^{2+} concentration (Berridge, 1993). $InsP_3$-induced Ca^{2+} release is supported by a highly specialized ion channel, the inositol (1,4,5)-trisphosphate receptor ($InsP_3R$). $InsP_3Rs$ were biochemically purified and cloned, and functional properties of these channels were extensively studied (reviewed by Taylor and Richardson, 1991; Berridge, 1993; Furuichi et al., 1994; Bezprozvanny and Ehrlich, 1995). Type I $InsP_3R$ ($InsP_3R$-I) was initially purified (Supattapone et al., 1988) and cloned (Furuichi et al., 1989; Mignery et al., 1990) from rodent cerebellum. $InsP_3R$-I is a complex of four 2,749 amino acid subunits (Mignery et al., 1989; Maeda et al., 1991). Different splice variants of $InsP_3R$-I are expressed in specific regions of the brain, at different stages of neuronal development, and in nonneuronal tissues (Nakagawa et al., 1991*a*, 1991*b*). After initial characterization of $InsP_3R$-I, multiple isoforms of $InsP_3R$ cDNA have been identified (reviewed by Furuichi et al., 1994).

Functional properties of the $InsP_3R$ have been characterized using Ca^{2+} flux measurements or planar lipid bilayer recordings (reviewed by Bezprozvanny and Ehrlich, 1995). The majority of functional studies were performed with cerebellar or vascular smooth muscle $InsP_3R$ isoforms, corresponding to splice variants of $InsP_3R$-I (Islam et al., 1996). $InsP_3R$ is a relatively nonselective cation channel (Bezprozvanny and Ehrlich, 1994), with conduction properties similar to that of ryanodine receptor (RyanR), another intracellular Ca^{2+} release channel. The central signaling role of $InsP_3R$ is highlighted by multiple levels of its modulation. Activity of $InsP_3R$ is affected by phosphorylation (reviewed by Ferris and Snyder, 1992), allosterically modulated by

Drs. Kaznacheyeva and Lupu contributed equally to this work and should be considered co-first authors.

Address correspondence to Dr. Ilya Bezprozvanny, Department of Physiology, K4.112, UT Southwestern Medical Center at Dallas, Dallas, TX 75235-9040. Fax: 214-648-8685; E-mail: bezprozv@utsw.swmed.edu

[1]*Abbreviations used in this paper:* $InsP_3R$, inositol (1,4,5)-trisphosphate receptor; RyanR, ryanodine receptor.

ATP (Ferris et al., 1990; Iino, 1991; Bezprozvanny and Ehrlich, 1993), and display bell-shaped Ca^{2+} dependence (Iino, 1990; Bezprozvanny et al., 1991; Finch et al., 1991). Putative structural determinants responsible for the $InsP_3R$ modulation have been identified using biochemical methods (reviewed by Furuichi et al., 1994).

Until now, structural and functional studies of the $InsP_3R$ largely proceed in parallel, with most of the functional work performed with the native $InsP_3R$ and recombinant $InsP_3R$ characterized mainly by biochemical methods. The main obstacle to further understanding $InsP_3R$ structure–function has been the lack of a convenient functional assay of expressed $InsP_3R$ activity. Recently, skeletal isoform of another intracellular Ca^{2+} release channel, RyanR, has been successfully expressed in HEK-293 and Chinese hamster ovary cell lines (Bhat et al., 1997; Chen et al., 1997). Basic single channel properties of recombinant skeletal RyanR were characterized using the planar lipid bilayer reconstitution assay (Bhat et al., 1997; Chen et al., 1997). We took a similar approach and set out to establish an assay of recombinant $InsP_3R$ function by combining planar lipid bilayer reconstitution technique with transient expression of neuronal rat $InsP_3R$-I cDNA in HEK-293 cells. We achieved high level functional expression of $InsP_3R$-I in HEK-293 cells and compared most basic functional properties of recombinant $InsP_3R$-I with the analogous properties of native rat cerebellar $InsP_3R$. Successful functional expression of $InsP_3R$ in heterologous expression systems provides an opportunity for future detailed structure–function characterization of this vital protein.

MATERIALS AND METHODS

$InsP_3R$-I Expression Methods

The full length neuronal rat $InsP_3R$-I cDNA clone in pCMV expression vector (pCMVI-9) (Mignery et al., 1990) was generously provided by Dr. Thomas Südhof (HHMI, Department of Molecular Genetics, UT Southwestern Medical Center at Dallas). This clone corresponds to SI− SII+ splice variant of $InsP_3R$-I (Mignery et al., 1990). We confirmed the fact that our working $InsP_3R$-I clone is indeed SI− SII+ by sequencing corresponding regions. To increase efficiency of $InsP_3R$-I expression in HEK-293 cells, $InsP_3R$-I coding sequence was subcloned into pcDNA3 (Invitrogen Corp., San Diego, CA) expression vector and 5′ untranslated region of the original pCMVI-9 clone was substituted with the Kozak consensus sequence (Kozak, 1987). To achieve this, we (*a*) subcloned a 7.9-kb Acc65I/XbaI fragment of pCMVI-9 into Acc65I/XbaI-digested pcDNA3 vector ($InsP_3R$-pcDNA3-A/X); (*b*) amplified the 5′ end of the rat $InsP_3R$-I clone by 15 cycles of PCR using high fidelity enzyme PfuI (Stratagene Inc., La Jolla, CA) with CGG GGT ACC GCC ACC ATG TCT GAC AAA ATG TCT A and CCG AAC CTC AGC AGG AGA AAC pair of primers. The resulting 1.3-kb PCR fragment was isolated, digested with KpnI, and cloned into KpnI-digested and -dephosphorylated $InsP_3R$-pcDNA3-A/X clone. The correct orientation of PCR fragment insertion into the KpnI site was verified by PCR using the same pair of primers, and the 5′ end of the clone with correct orientation of the fragment was sequenced from ATG to the KpnI site (1,255) in both directions to rule out the possibility of mutations introduced at the PCR step. The resulting construct ($InsP_3R$-pcDNA3) was used in HEK-293 cell transfection experiments. Some of the experiments were performed with $InsP_3R$-pCEP4 clone, constructed in a similar way except that pCEP4 expression vector (Invitrogen Corp.) was used instead of pcDNA3.

Human embryonic kidney cells (HEK-293, ATCC accession No. CRL-1573) were chosen for heterologous expression of $InsP_3R$. HEK-293 cells could be transfected by standard calcium-phosphate method with high efficiency and were used previously for functional expression of RyanR (Chen et al., 1997). HEK-293 cells were maintained in high glucose DMEM supplemented with 10% heat-inactivated fetal bovine serum and penicillin:streptomycin mixture (all from GIBCO BRL, Gaithersburg, MD). Cells were maintained in a tissue culture incubator at 37°C under 5% CO_2. 1 d before transfection, HEK-293 cells in an exponential growth phase were subcultured into large (75 cm^2) culture flasks using trypsin-EDTA treatment. On the next day, HEK-293 cells at ~50% confluence were transfected with $InsP_3R$-pcDNA3 DNA using the calcium phosphate method (MBS kit; Stratagene Inc.) or Lipofectamine reagent (GIBCO BRL) according to the manufacturer's suggestions and returned to the tissue culture incubator for several days to allow $InsP_3R$-I expression. Control HEK-293 cells were transfected by pcDNA3 DNA following identical protocols.

Microsomal Preparation

Rat cerebellar microsomes were isolated essentially as described previously for canine preparation (Bezprozvanny et al., 1991; Bezprozvanny and Ehrlich, 1993, 1994). Briefly, cerebellar microsomes were excised from 12 Sprague Dawley rats (4–5-wk old) that were killed by carbon dioxide inhalation and decapitated. Cerebellar microsomes were minced and manually homogenized on ice using Teflon/glass tissue homogenizer in 15 ml of homogenization buffer (5 mM NaN_3, 1 mM EDTA, 20 mM HEPES, pH 7.4) supplemented with the protease inhibitors cocktail (2 μg/ml aprotinin, 1 μg/ml leupeptin, 1 mM benzamidine, 0.2 mM γ-(2-aminoethyl)-benzenesulfonyl fluoride (AEBSF), 10 μg/ml pepstatin, 0.1 mg/ml PMSF). Another 15 ml of homogenization buffer was added to the homogenate, and the suspension was centrifuged for 15 min at 4,000 *g* (J 25.50 rotor; Beckman Instruments, Inc., Fullerton, CA). The supernatant fluid was filtered through cheesecloth, and the filtrate was centrifuged for 30 min at 90,000 *g* (Ti 50.2 rotor; Beckman Instruments, Inc.). The pellet from the latter spin was resuspended in 30 ml of high salt buffer B (0.6 M KCl, 5 mM NaN_3, 20 mM $Na_4P_2O_7$, 1 mM EDTA, 10 mM HEPES, pH 7.2) using Teflon/glass manual homogenizer and centrifuged for 15 min at 4,000 *g* (J 25.50 rotor). The resulting supernatant fluid was centrifuged for 30 min at 90,000 *g* (Ti 50.2 rotor). The pellet from the last spin was resuspended in 0.5 ml of storage buffer (10% sucrose, 10 mM MOPS, pH 7.0), aliquoted, snap frozen in liquid nitrogen, and stored at −80°C for future experiments. Total microsomal protein concentration (Bradford assay, BioRad kit; Bio-Rad Laboratories, Richmond, CA) in rat cerebellar microsomal preparation was typically close to 5 mg/ml.

Microsomes from HEK-293 cells were prepared by modification of the procedure described above for rat cerebellar microsomes. Briefly, 48 h after transfection with DNA, HEK-293 cells were loaded with 10 μM BAPTA-AM following standard protocol (Molecular Probes, Inc., Eugene, OR) and kept in serum-free DMEM overnight. On the next day, the HEK-293 cells were collected from two large (75 cm^2) culture flasks using trypsin-EDTA treatment, washed with PBS, and pelleted by centrifugation at 4°C for 5 min at 3,000 rpm (GH 3.8 rotor; Beckman Instruments). The cellular pellet was resuspended in 2.5 ml homogeni-

zation buffer A (5 mM NaN_3, 1 mM EDTA, 50 mM Tris-HCl, pH 8.0) supplemented with protease inhibitors cocktail and incubated on ice for 20 min. After incubation, cells were manually homogenized on ice with teflon-glass homogenizer, and 2.5 ml of homogenization buffer B (0.5 M sucrose, 1 mM EDTA, 20 mM HEPES, pH 7.5) was added. Cells were rehomogenized with teflon-glass homogenizer and centrifuged for 15 min at 3,000 rpm (GH 3.8 rotor). Concentrated high salt buffer (5×) was added to the supernatant to yield 0.6 M KCl and 20 mM $Na_4P_2O_7$. Microsomes were incubated on ice for 30 min and centrifuged for 15 min at 3,000 rpm (GH 3.8 rotor). The resulting supernatant was centrifuged for 30 min at 100,000 *g* (52,000 rpm, Ti 100.3 rotor; Beckman Instruments). The pellet from the last spin was resuspended in 0.15 ml storage buffer (10% sucrose, 10 mM MOPS, pH 7.0), aliquoted, quickly frozen in liquid nitrogen, and stored at −80°C. The microsomal protein concentration in HEK-293 microsomal preparation was typically close to 6 mg/ml.

Immunological Detection of $InsP_3R$-I

Peptide (RIGLLGHPPHMNVNPQQPA) corresponding to the carboxy terminus of rat $InsP_3R$-I (Mignery et al., 1990) was synthesized (Biopolymers Facility, HHMI, UT Southwestern Medical Center at Dallas) and coupled to keyhole limpet hemocyanin by glutaraldehyde treatment (Harlow and Lane, 1988). Two New Zealand White rabbits were immunized with the resulting antigenic conjugate mixed with Freund's complete adjuvant and boosted with the same antigen mixed with Freund's incomplete adjuvant 3 and 6 wk after initial immunization. Serum from the rabbit that had a higher titer of specific antibody was collected to yield a stock of anti–$InsP_3R$-I antibody (T_{443}). For analysis, microsomal proteins were solubilized in SDS (sodiumdodecyl sulfate) gel loading buffer, resolved by SDS-PAGE electrophoresis (6% polyacrylamide), and transferred to PVDF (polyvinylidene difluoride) membrane. Western blotting with T_{443} antibody was performed using the Western Max detection kit (Amresco Inc., Solon, OH) according to manufacturer's protocol. Titer and specificity of T_{443} antibody were determined to be similar to that of previously reported T_{210} anti–$InsP_3R$-I antibody (Mignery et al., 1989), generated against the same COOH-terminal fragment of rat $InsP_3R$-I. T_{210} antibody was a kind gift of Dr. Thomas Südhof.

Immunostaining of transfected HEK-293 cells with T_{443} antibody was performed according to standard protocol (Harlow and Lane, 1988). Briefly, transfected HEK-293 cells were grown on glass coverslips in tissue culture incubator (37°C, 5% CO_2) for 24 h. Cells were fixed with 4% paraformaldehyde and permeabilized with 0.1% Triton X-100. Nonspecific antibody binding sites were blocked by Fraction V bovine serum albumin and stained with T_{443} antibody diluted 1:1,000 in the blocking solution. Bound T_{443} antibodies were visualized with rhodamine-conjugated anti–rabbit IgG (Jackson Immunoresearch Laboratories, Inc., West Grove, PA) and mounted on microscopic slides with Aqua-Mount (Lerner Labs) media for fluorescent microscopy (Axiovert 135, 20× objective; Carl Zeiss, Inc., Thornwood, NY) or laser (Argon/Krypton) confocal immunofluorescence microscopy (MRC-1024; Bio-Rad Laboratories; attached to an Axiovert 135, 60× oil-immersed objective; Carl Zeiss, Inc.).

[^{3}H]$InsP_3$ Binding

Specific [^{3}H]$InsP_3$ (Amersham Corp., Arlington Heights, IL) binding to microsomes isolated from HEK-293 cells or rat cerebellar microsomes was measured with minor modifications of procedure described previously (Chadwick et al., 1990). Briefly, microsomes (5 μg protein) were incubated on ice with 10 nM [^{3}H]$InsP_3$ in the binding buffer (50 mM Tris-HCl, pH 9.0, 1 mM EDTA, 1 mM DTT, 100 mM NaCl) and precipitated with 12.5% PEG and 1.2 mg/ml γ-globulin at 14,000 *g*. Precipitates were quickly washed with the binding buffer, dissolved in Soluene, and their [^{3}H] content was determined by liquid scintillation counting. Nonspecific counts, determined in the presence of 25 μM nonlabeled $InsP_3$, were subtracted from the total to yield specific binding. The density of specific $InsP_3$ binding sites was determined by normalization of obtained results for specific [^{3}H]$InsP_3$ radioactivity and the amount of microsomal protein in the assay. Scatchard analysis of specific $InsP_3$ binding sites in microsomal preparations was done by adding variable amounts of $InsP_3$ (from 10 nM to 8 μM concentrations) to [^{3}H]$InsP_3$ binding experiments performed as described.

Planar Lipid Bilayer Recordings and Single-Channel Data Analysis

Planar lipid bilayers were formed from PE (phosphatidylethanolamine):PS (phosphatidylserine) (3:1) synthetic lipid (Avanti Polar Lipids, Alabaster, AL) mixture in decane on the small (100–200-μm diameter) hole in Teflon film separating two chambers 3 ml each (*cis* and *trans*). Before formation of the bilayer, the hole was prepainted with PC (phosphatidylcholine):PS mixture (3:1). Recombinant $InsP_3R$-I from HEK-293 cells or rat cerebellar $InsP_3R$ were incorporated into the bilayer by microsomal vesicle fusion as described previously for canine preparation (Bezprozvanny et al., 1991; Bezprozvanny and Ehrlich, 1993, 1994). Single channel currents were recorded at 0-omV transmembrane potential using 50 mM Ba^{2+} dissolved in HEPES, pH 7.35, in the *trans* (intraluminal) side as a charge carrier (Bezprozvanny and Ehrlich, 1994). In most experiments (standard recording conditions of $InsP_3R$ activity), the *cis* (cytosolic) chamber contained 110 mM Tris dissolved in HEPES, pH 7.35, 0.2 μM free Ca^{2+} (Bezprozvanny et al., 1991) buffered with 1 mM EGTA and 0.7 mM $CaCl_2$, 1 mM Na_2ATP (Bezprozvanny and Ehrlich, 1993), and 2 μM $InsP_3$. We found that 2 μM of ruthenium red in the *cis* chamber increases native and recombinant $InsP_3R$ single channel open probability (P_o) 1.5–2-fold (Lupu and Bezprozvanny, manuscript in preparation). Thus, in most experiments, channels were recorded in the presence of 2 μM of ruthenium red in the *cis* chamber to stimulate $InsP_3R$ activity and inhibit cerebellar RyanR (Bezprozvanny et al., 1991). All additions ($InsP_3$, ATP, $CaCl_2$, heparin) were to the *cis* chamber from the concentrated stocks with at least 30 s stirring of solutions in both chambers.

$InsP_3R$ single channel currents were amplified (OC-725; Warner Instruments, Hamden, CT), filtered at 1 kHz by a low pass eight-pole Bessel filter, digitized at 5 kHz (Digidata 1200; Axon Instruments, Foster City, CA) and stored on computer hard drive and recordable optical discs. Single channel data for off-line computer analysis (pClamp 6.0.3; Axon Instruments) were filtered digitally at 500 Hz and, for presentation of the current traces data, were filtered at 200 Hz. P_o was determined using half-threshold crossing criteria ($t \geq 2$ ms) from records lasting at least 2.5 min.

RESULTS

Transient Expression of $InsP_3R$ in HEK-293 Cell Line

Transfection of HEK-293 cell line with $InsP_3R$-pcDNA3 clone resulted in transient expression of $InsP_3R$-I in 20–30% of transfected cells as determined by immunocytochemical staining with T_{443} anti–$InsP_3R$-I polyclonal antibody (Fig. 1 *A*). No detectable staining with T_{443} antibody was observed in untransfected HEK-293 cells (data not shown) or cells transfected with pcDNA3 vec-

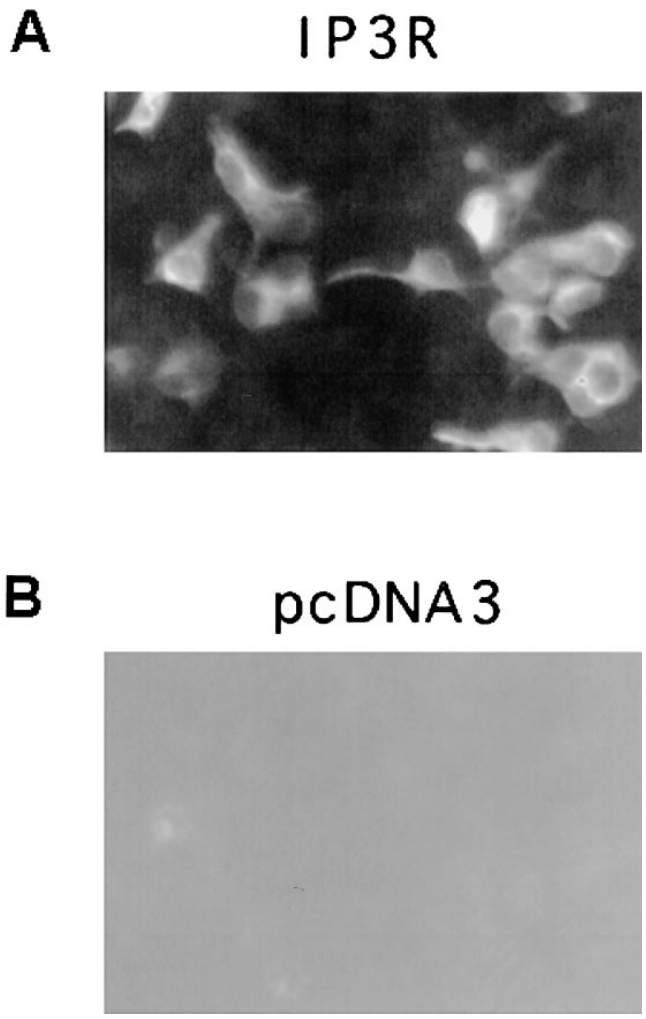

FIGURE 1. Immunocytochemical staining of transfected HEK-293 cells with the anti–$InsP_3R$-I antibody. HEK-293 cells were transfected with $InsP_3R$-pcDNA3 clone (*A*) or pcDNA3 vector alone (*B*). Expressed $InsP_3R$-I receptors were detected by immunocytochemical staining using T_{443} antibody and rhodamine-conjugated anti–rabbit IgG. Immunostaining and fluorescent imaging was performed as described in MATERIALS AND METHODS using 20× objective. Fluorescent signal was monitored on rhodamine channel.

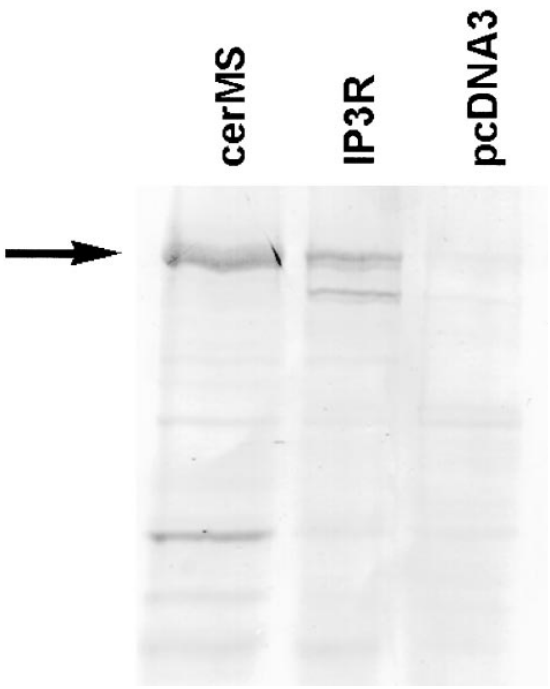

FIGURE 2. Western blot of microsomal proteins with the anti–$InsP_3R$-I antibody. Rat cerebellar microsomes (*cerMS*) and microsomes isolated from HEK-293 cells transfected with $InsP_3R$-pcDNA3 (*IP3R*) or with expression vector alone (*pcDNA3*) were analyzed by Western blotting with T_{443} antibody as described in MATERIALS AND METHODS. For each microsomal preparation, 20 μg total protein was loaded on the gel. The arrow points to the 260-kD position expected for $InsP_3R$.

tor alone (Fig. 1 *B*). At the subcellular level, expressed $InsP_3R$ was localized to cytoplasmic (presumably endoplasmic reticulum) and perinuclear regions of transfected HEK-293 cells as determined using laser confocal fluorescent microscopy (data not shown). Observed subcellular distribution of $InsP_3R$ expressed in HEK-293 cells was similar to that reported previously for $InsP_3R$ expressed heterologously in COS cells (Takei et al., 1994).

Quantification of $InsP_3R$ Expression in HEK-293 Cells

Endoplasmic reticulum–enriched microsomal preparation was isolated from HEK-293 cells 72 h after transfection with $InsP_3R$-pcDNA3 or pcDNA3 as described in MATERIALS AND METHODS. A major band was recognized on Western blots with T_{443} anti–$InsP_3R$-I antibody in microsomes extracted from $InsP_3R$-pcDNA3–transfected cells (Fig. 2), whereas the signal was very faint in membranes obtained from pcDNA3-transfected HEK-293 cells (Fig. 2) or untransfected HEK-293 cells (data not shown). The position of the band detected by T_{443} antibody in microsomes from $InsP_3R$-pcDNA3–transfected HEK-293 cells corresponds to the expected position of full-length rat $InsP_3R$-I (~260 kD; Fig. 2, *arrow*) and to the position of the band detected by T_{443} antibody in rat cerebellar microsomes loaded on the same gel. Shorter immunoreactive products apparent in both lanes most likely result from limited proteolysis of $InsP_3R$ during microsomal extraction from HEK-293 cells and rat cerebellum. Based on relative density of major immunoreactive bands (Fig. 2), we estimated that $InsP_3R$-I in microsomes from $InsP_3R$-pcDNA3–transfected HEK-293 cells are at least 10-fold more abundant than in HEK-293 cells transfected with pcDNA3 alone. The density of $InsP_3R$-I in rat cerebellar microsomes is approximately twofold higher than in microsomes from $InsP_3R$-pcDNA3–transfected HEK-293 cells (Fig. 2).

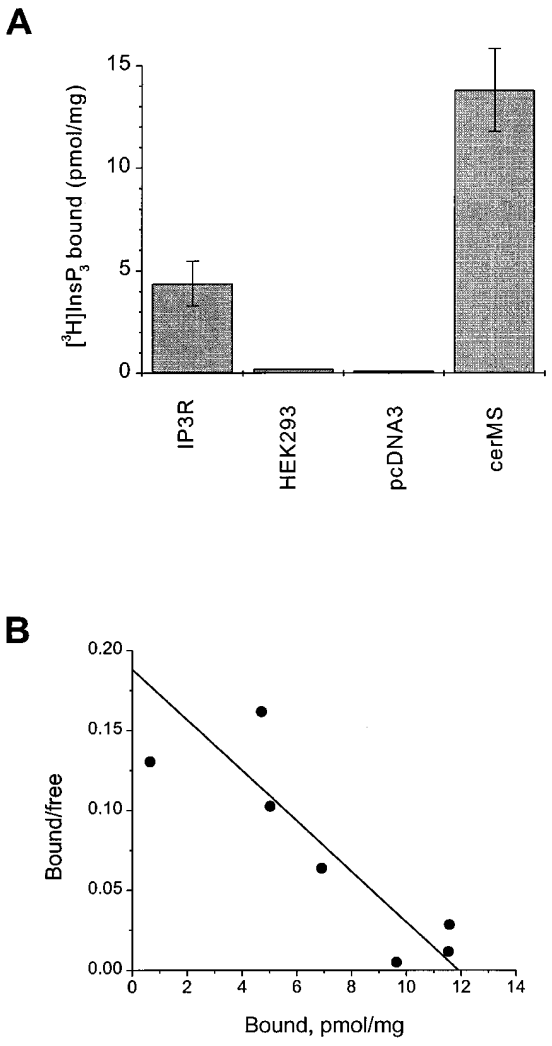

FIGURE 3. Specific [^{3}H]$InsP_3$ binding sites are expressed in $InsP_3$R-pcDNA3–transfected HEK-293 cells. (*A*) Density of specific [^{3}H]$InsP_3$ binding sites in microsomal preparations isolated from $InsP_3$R-pcDNA3–transfected HEK-293 cells (*IP3R*, $n = 6$), from the untransfected cells (*HEK293*), from the cells transfected with the expression vector alone (*pcDNA3*), and from the rat cerebellar microsomes (*cerMS*, $n = 10$). Microsomal preparation and [^{3}H]$InsP_3$ binding assay were performed as described in MATERIALS AND METHODS. The data shown are mean ± SEM. (*B*) Scatchard analysis of specific [^{3}H]$InsP_3$ binding sites present in microsomes isolated from $InsP_3$R-pcDNA3–transfected HEK-293 cells. Fit to the data (*line*) yields $K_d = 60$ nM $InsP_3$ and $B_{max} = 12$ pmol/mg.

$InsP_3$R-III is the major isoform expressed in most cultured cell lines (De Smedt et al., 1997). T_{443} antibody, raised against carboxy-terminal peptide fragment of $InsP_3$R-I (see MATERIALS AND METHODS), may not recognize most of the endogenous $InsP_3$R present in HEK-293 cells. For better comparison of $InsP_3$R-I expression level with endogenous $InsP_3$R, we used quantitative [^{3}H]$InsP_3$ binding assay as described in MATERIALS AND METHODS. At 10 nM [^{3}H]$InsP_3$, the density of specific $InsP_3$ binding sites was determined to be no more than 0.2 pM/mg in untransfected HEK-293 cells or HEK-293 cells transfected with pcDNA3 vector (Fig. 3 *A*). The density of specific [^{3}H]$InsP_3$ binding sites varied from 1.5 to 8 pmol/mg between different microsomal preparations from $InsP_3$R-pcDNA3–transfected HEK-293 cells, yielding an average value of 4.4 ± 1.1 pmol/mg ($n = 6$) (Fig. 3 *A*). Thus, transfection of HEK-293 cells with $InsP_3$R-pcDNA3 results in at least a 20-fold increase in $InsP_3$R density. For comparison, we determined the density of $InsP_3$R in rat cerebellar microsomes to be equal to 14 ± 2 pmol/mg ($n = 10$) (Fig. 3 *A*), 70-fold above endogenous background in HEK-293 cells and 3-fold higher than in microsomes from $InsP_3$R-pcDNA3–transfected HEK-293 cells. These data agree with results from T_{443} Western blotting (Fig. 2). When [^{3}H]$InsP_3$ binding to microsomes from $InsP_3$R-pcDNA3–transfected HEK-293 cells was characterized by Scatchard analysis (Fig. 3 *B*), affinity of specific $InsP_3$ binding sites equal to 60 nM was determined, similar to previously reported K_d values for the rat cerebellar $InsP_3$R (Worley et al., 1987) and the rat $InsP_3$R-I expressed in COS cells (Mignery et al., 1990).

We concluded that transient transfection of HEK-293 cells with the $InsP_3$R-pcDNA3 clone results in high level heterologous expression of rat neuronal $InsP_3$R. Expressed $InsP_3$R appears to be full length, has normal immunoreactive properties, and has the expected subcellular localization. Expressed $InsP_3$R retains its normal $InsP_3$ binding properties. The density of expressed $InsP_3$R is at least 20-fold higher than the density of endogenous $InsP_3$R present in HEK-293 cells, and only 2–3-fold lower than $InsP_3$R density in rat cerebellar microsomes.

Single-Channel Recording of Recombinant $InsP_3$R Expressed in HEK-293 Cells

High level heterologous expression of $InsP_3$R in HEK-293 cells provides an opportunity for characterization of single channel properties of recombinant $InsP_3$R. When microsomes isolated from $InsP_3$R-pcDNA3–transfected HEK-293 cells were fused to planar lipid bilayers, no channel activity was observed in control conditions (Fig. 4 *A*, *top*). Addition of 2 μM $InsP_3$ to the cytosolic (*cis*) compartment activated $InsP_3$-gated channels in the bilayers (Fig. 4 *A*). $InsP_3$-gated channels from $InsP_3$R-pcDNA3–transfected HEK-293 cells were inhibited by heparin (data not shown), in agreement with known $InsP_3$R pharmacological properties. $InsP_3$-gated channels were observed frequently (in 30 of 76 experiments) with microsomes from $InsP_3$R-pcDNA3–transfected HEK-293 cells, but did not appear in experiments with microsomes from untransfected HEK-293 cells ($n = 4$) or pcDNA3-transfected HEK-293 cells ($n = 5$). We did not observe $InsP_3$-gated channels in experiments with microsomes from pCMVI-9-transfected HEK-

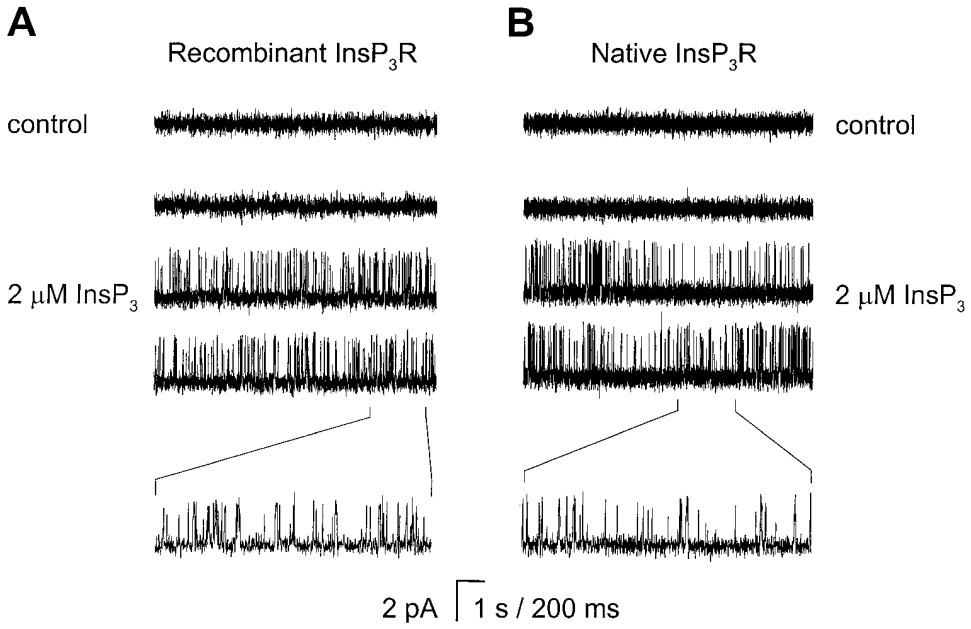

FIGURE 4. Single channel records of recombinant $InsP_3R$ and native rat cerebellar $InsP_3R$ in planar lipid bilayers. Representative single channel currents through recombinant rat $InsP_3R$ (*A*) and native rat cerebellar $InsP_3R$ (*B*). Control traces were obtained in the presence of 0.2 μM Ca^{2+} and 1 mM Na_2ATP. Addition of 2 μM $InsP_3$ on the *cis* (cytosolic) side evoked openings of recombinant $InsP_3R$-I and native rat cerebellar $InsP_3R$. Current traces at the expanded time scale are shown on the bottom. Similar results were obtained with 7 independent microsomal preparations from $InsP_3R$-I-transfected HEK-293 cells and 10 rat cerebellar microsomal preparations. $InsP_3R$-gated channels were not observed in similar reconstitution experiments with microsomes from untransfected HEK-293 cells or from HEK-293 transfected with pcDNA3 vector alone.

293 cells (Mignery et al., 1990; $n = 5$), presumably due to low $InsP_3R$ expression levels with this construct (we detected only ~0.3 pmol/mg specific [^{3}H]$InsP_3$ binding sites in microsomes isolated from pCMVI-9-transfected HEK-293 cells). We also observed strong correlation between the efficiency of $InsP_3R$-pcDNA3 transfections of HEK-293 cells (as judged by the density of specific [^{3}H]$InsP_3$ binding sites) and the frequency of $InsP_3$-gated channels' appearance in planar lipid bilayer experiments. Indeed, occurrence of $InsP_3$-gated channels in bilayers varied from 25% (6 of 24) for less optimal transfection experiments (2 pmol/mg specific [^{3}H]$InsP_3$ binding sites in microsomal preparation) to 51% (25 of 49) in more successful transfections (8 pmol/mg specific [^{3}H]$InsP_3$ binding sites), comparable to the success rate of $InsP_3R$ incorporation in experiments with rat cerebellar microsomes (typically ~60% for most cerebellar microsomal preparations). No channel activity was observed in experiments with microsomes that had a density of [^{3}H]$InsP_3$ binding sites of <2 pmol/mg. All these data lead to the conclusion that endogenous $InsP_3R$ background (no more than 0.2 pmol/mg [^{3}H]$InsP_3$ binding sites) is negligible in our planar lipid bilayer assay, and $InsP_3$-gated channels observed in these experiments correspond to the activity of recombinant $InsP_3R$-I expressed in HEK-293 cells.

Rodent cerebellar $InsP_3R$ corresponds to $InsP_3R$-I SII+ splice isoform, which is 85% SI− and 15% SI+ (Nakagawa et al., 1991*a*). Thus, our working clone $InsP_3R$-pcDNA3 ($InsP_3R$-I, SI− SII+, see MATERIALS AND METHODS) corresponds to predominant $InsP_3R$ isoform expressed in rodent cerebellum. It is interesting to compare single channel properties of recombinant rat $InsP_3R$-I with characteristics of native rat cerebellar $InsP_3R$. To perform this comparison, we isolated rat cerebellar microsomes (see MATERIALS AND METHODS) and fused them to planar lipid bilayers. The addition of 2 μM $InsP_3$ to the cytosolic compartment resulted in $InsP_3$-gated channel activity (Fig. 4 *B*), which was inhibited by heparin (data not shown). Thus, rat cerebellar $InsP_3R$ activity could be recorded in planar lipid bilayers by using an experimental protocol similar to one used previously for canine cerebellar $InsP_3R$ single-channel recordings (Bezprozvanny et al., 1991; Bezprozvanny and Ehrlich, 1993, 1994).

Detailed comparison of functional properties of recombinant $InsP_3R$-I and native rat cerebellar $InsP_3R$ in the standard recording conditions (0.2 μM free Ca^{2+}, 1 mM ATP, 2 μM $InsP_3$ on the *cis* side of the membrane; 50 mM Ba^{2+} on the *trans* side as a current carrier) was performed. Fig. 5 compares the results of single channel data analysis obtained in representative experiments with recombinant $InsP_3R$-I (*top*) and native rat cerebellar $InsP_3R$ (*bottom*). Similar data from three independent experiments with recombinant $InsP_3R$-I (rec $InsP_3R$-I) and native rat cerebellar $InsP_3R$ (cer $InsP_3R$) were averaged together to generate Table I. Open dwell time distribution of recombinant and native $InsP_3R$ could be fit with a single exponent yielding the mean open time τ_o (Fig. 5, Table I). Closed dwell

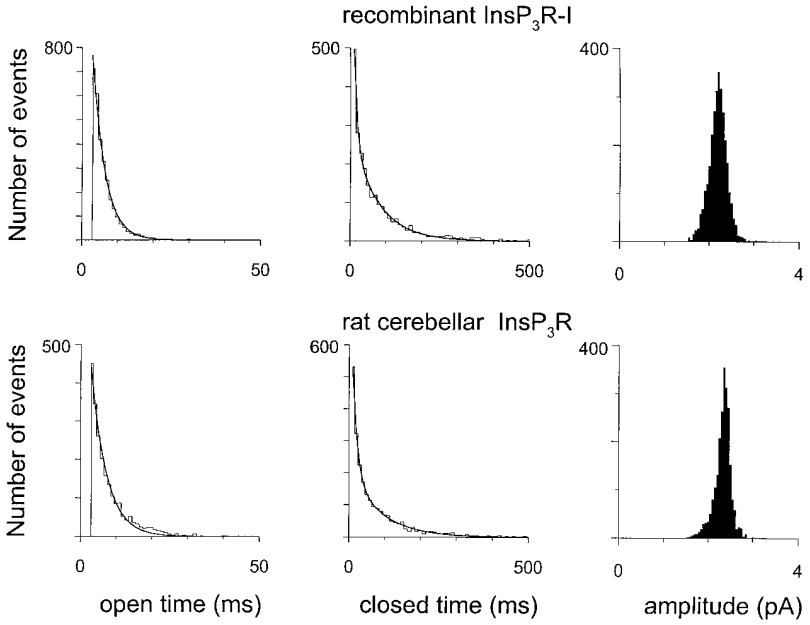

FIGURE 5. Analysis of the single channel records obtained with recombinant rat $InsP_3R$ (*top*) and native rat cerebellar $InsP_3R$ (*bottom*). Open (*left*) and closed (*center*) dwell time distributions and unitary current histogram (*right*) are shown. Open time distributions were fit with a single exponential function (*curve*) that yielded a τ_o of 3.45 ms for recombinant $InsP_3R$-I and 4.2 ms for native cerebellar $InsP_3R$. The sum of two exponentials (*curves*) was used to fit closed-time distributions (see text). The corresponding time constants were τ_{c1} of 18.4 ms and τ_{c2} of 96.5 ms for recombinant $InsP_3R$-I; τ_{c1} of 13.4 ms and τ_{c2} of 99.3 ms for native rat cerebellar $InsP_3R$. Unitary currents were fitted with a Gaussian function that was centered at 2.17 pA for recombinant $InsP_3R$-I and at 2.33 pA for the native rat cerebellar $InsP_3R$. The figure was generated with the data from the same experiments as shown on Fig. 4. Similar analysis of three independent experiments with recombinant $InsP_3R$ and native rat cerebellar $InsP_3R$ was performed to generate Table I.

time distribution for expressed $InsP_3R$-I and native cerebellar $InsP_3R$ could be fit better with a sum of two exponential functions: $W_1 \exp(-t/\tau_{c1}) + W_2 \exp(-t/\tau_{c2})$ (Fig. 5). Average values of time constants, τ_{c1} and τ_{c2}, and relative weight factors, W_1 and W_2, are in Table I. Single channel current amplitude histograms for both types of channels were fit with a single Gaussian function that yielded mean size of the single channel current at 0 mV transmembrane voltage *i* (Fig. 5, Table I). From current measurement at different transmembrane potentials, single channel conductance γ of recombinant $InsP_3R$-I and native rat cerebellar $InsP_3R$ in the standard recording conditions was close to 80 pS (Fig. 6, Table I). Thus, we concluded that most fundamental gating and conduction properties of recombinant neuronal rat $InsP_3R$-I heterologously expressed in HEK-293 cells are not significantly different from analogous characteristics of native rat cerebellar $InsP_3R$.

Bell-shaped Ca^{2+} Dependence of Recombinant $InsP_3R$ Expressed in HEK-293 Cells

Bell-shaped dependence of $InsP_3R$ on cytosolic Ca^{2+} is one of the most fundamental $InsP_3R$ properties responsible for complex spatiotemporal aspects of Ca^{2+} signaling (Berridge, 1993). It is not known if Ca^{2+} interacts directly with the $InsP_3R$ or if some auxiliary Ca^{2+}-binding protein is required to confer Ca^{2+} sensitivity to $InsP_3R$. To address this question, we analyzed modulation of recombinant $InsP_3R$ by cytosolic Ca^{2+} in planar lipid bilayer reconstitution experiments. We monitored recombinant $InsP_3R$ activity in bilayers in the presence of 2 μM $InsP_3$ and 1 mM Na_2ATP at *cis* (cytosolic) Ca^{2+} concentrations in the range between 10 nM and 5 μM Ca^{2+}. Ca^{2+} concentration in the *cis* chamber, calculated according to Fabiato (1988), was adjusted by using calibrated 20 mM $CaCl_2$ stock solution and 1 mM mixture of HEDTA and EGTA. We determined that recombinant $InsP_3R$ expressed in HEK-293 cells retained bell-shaped dependence on cytosolic Ca^{2+} concentration (Fig. 7, $n = 3$), which was similar to Ca^{2+} dependence of

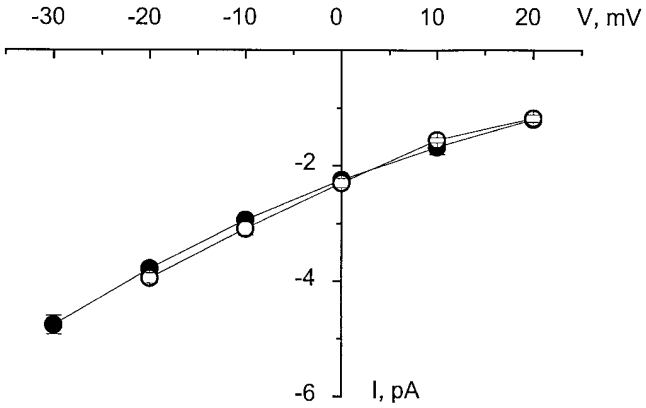

FIGURE 6. Current–voltage relationship of recombinant $InsP_3R$ (●) and native rat cerebellar $InsP_3R$ (○). Activity of recombinant and native $InsP_3R$ was recorded in planar lipid bilayers as described in MATERIALS AND METHODS in the range of transmembrane potentials from −30 to +20 mV. Single channel current amplitude at each voltage was determined from Gaussian fit, and then data from different experiments were averaged together. The data obtained at each voltage are shown as mean ± SEM ($n = 3$ for recombinant $InsP_3R$; $n = 2$ for native rat cerebellar $InsP_3R$). Single channel slope conductance for recombinant $InsP_3R$ ($\gamma = 78$ pS) and for the native rat cerebellar $InsP_3R$ ($\gamma = 80$ pS) was determined from the linear fit to the corresponding set of data in the range of voltages between −20 and +10 mV.

TABLE I

Comparison of Basic Single Channel Properties of Recombinant Neuronal Rat $InsP_3R$ (rec $InsP_3R$) with the Native Rat Cerebellar $InsP_3R$ (cer $InsP_3R$)

$InsP_3R$ type	Open time τ_o (ms)	Closed time τ_{c1} (ms)	W_1 (%)	τ_{c2} (ms)	W_2 (%)	Current i (pA)	Conductance γ (pS)
	$n = 7$	$n = 3$				$n = 3$	$n = 3$
rec $InsP_3R$	3.5 ± 0.2	18 ± 2	32 ± 11	129 ± 29	68 ± 11	2.21 ± 0.02	78 ± 0.9
cer $InsP_3R$	4.2 ± 0.5	17 ± 3	29 ± 7	190 ± 90	71 ± 7	2.25 ± 0.05	80 ± 2.0

native canine (Bezprozvanny et al., 1991) and rat (data not shown) cerebellar $InsP_3R$. Recombinant $InsP_3R$ was also allosterically modulated by ATP (data not shown), similar to native cerebellar $InsP_3R$ (Bezprozvanny and Ehrlich, 1993).

DISCUSSION

In this paper, we report transient expression of neuronal rat $InsP_3R$ ($InsP_3R$-I, SI− SII+ splice isoform) (Mignery et al., 1990) in HEK-293 cell line and characterize basic functional properties of recombinant $InsP_3R$-I at the single channel level. We compared properties of recombinant $InsP_3R$ expressed in HEK-293 cells with rat cerebellar $InsP_3R$. Rodent cerebellar $InsP_3R$ corresponds to $InsP_3R$-I SII+ splice isoform, which is 85% SI− and 15% SI+ (Nakagawa et al., 1991*a*). $InsP_3R$ expressed in HEK-293 cells were specifically recognized by rabbit polyclonal antibody raised against rat $InsP_3R$-I carboxy terminus. Recombinant $InsP_3R$ had normal (~260 kD) mobility on SDS-PAGE gel, and expected mobility for intracellular Ca^{2+} release channel subcellular localization to endoplasmic reticulum and perinuclear region. Expressed $InsP_3R$ retained specific $InsP_3$ binding activity with a K_d of 60 nM, similar to the native cerebellar $InsP_3R$. Based on immunological assays and quantitative [^{3}H]$InsP_3$ binding experiments, the estimated density of recombinant $InsP_3R$-I in microsomes extracted from $InsP_3R$-pcDNA3–transfected HEK-293 cells was at least 20-fold above endogenous $InsP_3R$ background and 2–3-fold lower than the $InsP_3R$ density in rat cerebellar microsomes. When incorporated into planar lipid bilayers, the recombinant rat $InsP_3R$-I formed functional $InsP_3$-gated Ca^{2+} channels very similar in their gating and conduction properties to native rat cerebellar $InsP_3R$. Channel properties of recombinant rat $InsP_3R$-I were also very similar to the properties of canine cerebellar $InsP_3R$, previously characterized in detail (Bezprozvanny and Ehrlich, 1994). Similar to native cerebellar $InsP_3R$, recombinant $InsP_3R$-I displayed bell-shaped dependence on cytosolic Ca^{2+} concentration (Bezprozvanny et al., 1991) and was allosterically modulated by ATP (Bezprozvanny and Ehrlich, 1993).

The background from endogenous $InsP_3R$ present in HEK-293 was insignificant in planar lipid bilayer assay, most likely due to 20-fold molar excess of recombinant $InsP_3R$. This is a main advantage of the planar lipid bilayer reconstitution method as it enabled us to treat HEK-293 cells as "zero background" host. From our experience, the microsomal density of $InsP_3R$ of at least 2 pmol/mg is required for successful $InsP_3R$ reconstitution into bilayers, 10-fold higher than the density of endogenous $InsP_3R$ in microsomes isolated from HEK-293 cells. In comparison, Ca^{2+} flux assay is affected by endogenous $InsP_3R$ background to a far greater extent, and endogenous $InsP_3R$ present in L-type mouse fibroblasts obscured previously published measurements of recombinant $InsP_3R$ activity using this method (Mi-

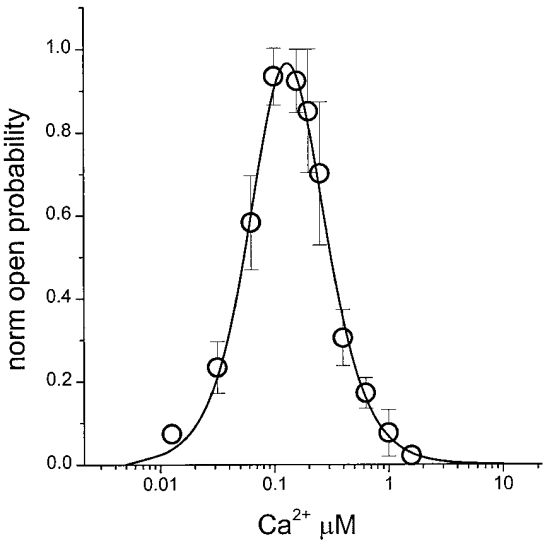

FIGURE 7. Bell-shaped Ca^{2+} dependence of recombinant $InsP_3R$. Recombinant $InsP_3R$ activity was measured in bilayers in the presence of 2 μM $InsP_3$ and 1 mM Na_2ATP at *cis* (cytosolic) Ca^{2+} concentrations in the range between 10 nM and 5 μM Ca^{2+}. Ca^{2+} concentration in the *cis* chamber, calculated according to Fabiato (1988), was adjusted by using calibrated 20 mM $CaCl_2$ stock solution and 1 mM mixture of HEDTA and EGTA. P_o in each experiment was normalized to maximum P_o observed in the same experiment, and then data from three independent experiments were averaged together at each Ca^{2+} concentration (○). Averaged data were fit by the bell-shaped equation (Bezprozvanny et al., 1991):

$$P = P_{max}\frac{k^n[Ca^{2+}]^n}{(k^n + [Ca^{2+}]^n)(K^n + [Ca^{2+}]^n)}.$$

Best fit to the data (*line*) yielded $k = 0.14$ μM Ca^{2+}, $K = 0.13$ μM Ca^{2+}, and $n = 2$.

yawaki at al., 1990). Thus, we concluded that $InsP_3$-gated channels recorded in our experiments with microsomes from $InsP_3$R-pcDNA3–transfected HEK-293 cells correspond to the activity of recombinant rat $InsP_3$R, which possess basic functional properties of native cerebellar $InsP_3$R. However, we cannot rule out the possibility that functional $InsP_3$-gated channel is formed from the complex of heterologously expressed neuronal rat $InsP_3$R-I with the auxiliary components recruited from the set of proteins endogenously present in HEK-293 cells.

Transient expression of rat and mouse $InsP_3$R-I cDNA has been previously reported using COS cells (Mignery et al., 1990) and the NG-108 cell line (Furuichi et al., 1989). Although recombinant $InsP_3$R-I obtained in these studies retain normal immunoreactivity and specific $InsP_3$ binding properties, it has not been demonstrated whether they form a functional $InsP_3$-gated Ca^{2+} channel. $InsP_3$-induced Ca^{2+} release is facilitated in the L-fibroblast stable cell line overexpressing mouse $InsP_3$R-I (Miyawaki et al., 1990). This result indicates that the $InsP_3$R-I expressed in L-fibroblasts are functional channels. Detailed characterization of recombinant $InsP_3$R-I functional properties has not been previously reported due to substantial background signal from endogenous $InsP_3$R in $InsP_3$-induced Ca^{2+} flux measurements. Thus, the present report constitutes the first description of basic functional properties of recombinant $InsP_3$R-I expressed in a heterologous system. We found that heterologous expression of $InsP_3$R-I cDNA in HEK-293 cells is sufficient to confer most basic functional properties of native cerebellar $InsP_3$R. Gating and conductance properties of recombinant $InsP_3$R-I are very similar to native rat cerebellar $InsP_3$R (Table I).

Similar to native cerebellar (Bezprozvanny et al., 1991; Finch et al., 1991) and smooth muscle (Iino, 1990) $InsP_3$R, recombinant $InsP_3$R-I displayed bell-shaped dependence on cytosolic Ca^{2+} concentration (Fig. 7). Supporting biphasic regulation of $InsP_3$R-I requires interaction of Ca^{2+} with both activating and inhibitory sites of $InsP_3$R. Ca^{2+} may bind directly to $InsP_3$R or act via auxiliary Ca^{2+} binding protein. If it exists, this auxiliary protein must be ubiquitously expressed to cause similar Ca^{2+} sensitivity of native cerebellar $InsP_3$R (Bezprozvanny et al., 1991) and recombinant $InsP_3$R expressed in HEK-293 cells (Fig. 7). One obvious candidate for this role is calmodulin (CaM). Indeed, biochemical analysis identified a unique CaM-binding site in the coupling domain of $InsP_3$R-I (Yamada et al., 1995). We hypothesize that CaM plays a role in biphasic modulation of $InsP_3$R by Ca^{2+}. Purified $InsP_3$R is no longer inhibited by Ca^{2+} (Callamaras and Parker, 1994), probably due to loss of CaM during the purification procedure. Thus, it is possible that CaM is responsible for the inhibitory part of the bell-shaped curve. This hypothesis, as well as other ideas related to structural determinants responsible for $InsP_3$R conductance and modulation by Ca^{2+} and ATP, can now be tested using methodology described in the present report.

In conclusion, functional expression of recombinant $InsP_3$R in HEK-293 cells provides a useful model for studies of functional differences between $InsP_3$R-I splice variants and $InsP_3$R isoforms, and in combination with site-directed mutagenesis of $InsP_3$R cDNA will lead to a better understanding of structural determinants responsible for most fundamental $InsP_3$R functional properties.

We are grateful to G. Mignery and T.C. Südhof for rat $InsP_3$R-I cDNA. We thank G. DeMartino and X. Lin for advice with rabbit polyclonal antibody production, K. Luby-Phelps and H.R. Payne for help with immunofluorescent microscopy and confocal imaging, and J. Ma and S.R.W. Chen for advice on transfection procedures and communicating their results before publication. I. Bezprozvanny is thankful to S. Bezprozvannaya for tremendous support and encouragement of his work. E. Kaznacheyeva is on leave from the Institute of Cytology, Russian Academy of Sciences (St. Petersburg, Russia).

Supported by the American Heart Association, Robert Welch Foundation, and start-up funds from UT Southwestern (to I. Bezprozvanny).

Original version received 30 December 1997 and accepted version received 26 March 1998.

REFERENCES

Berridge, M.J. 1993. Inositol trisphosphate and calcium signalling. *Nature.* 361:315–325.

Bezprozvanny, I., and B.E. Ehrlich. 1993. ATP modulates the function of inositol 1,4,5-trisphosphate-gated channels at two sites. *Neuron.* 10:1175–1184.

Bezprozvanny, I., and B.E. Ehrlich. 1994. Inositol (1,4,5)-trisphosphate ($InsP_3$)-gated Ca channels from cerebellum: conduction properties for divalent cations and regulation by intraluminal calcium. *J. Gen. Physiol.* 104:821–856.

Bezprozvanny, I., and B.E. Ehrlich. 1995. The inositol 1,4,5-trisphosphate ($InsP_3$) receptor. *J. Membr. Biol.* 145:205–216.

Bezprozvanny, I., J. Watras, and B.E. Ehrlich. 1991. Bell-shaped calcium-response curves of $Ins(1,4,5)P_3$- and calcium-gated channels from endoplasmic reticulum of cerebellum. *Nature.* 351: 751–754.

Bhat, M.B., J. Zhao, H. Takeshima, and J. Ma. 1997. Functional calcium release channel formed by the carboxyl-terminal portion of ryanodine receptor. *Biophys. J.* 73:1329–1336.

Callamaras, N., and I. Parker. 1994. Inositol 1,4,5-trisphosphate receptors in *Xenopus laevis* oocytes: localization and modulation by Ca^{2+}. *Cell Calcium.* 15:66–78.

Chadwick, C.C., A. Saito, and S. Fleischer. 1990. Isolation and char-

acterization of the inositol trisphosphate receptor from smooth muscle. *Proc. Natl. Acad. Sci. USA*. 87:2132–2136.

Chen, S.R.W., P. Leong, J.P. Imredy, C. Bartlett, L. Zhang, and D.H. MacLennan. 1997. Single-channel properties of the recombinant skeletal muscle Ca release channel (ryanodine receptor). *Biophys. J.* 73:1904–1912.

De Smedt, H., L. Missiaen, J.B. Parys, R.H. Henning, I. Sienaert, S. Vanlingen, A. Gijsens, B. Himpens, and R. Casteels. 1997. Isoform diversity of the inositol trisphosphate receptor in cell types of mouse origin. *Biochem. J.* 322:575–583.

Fabiato, A. 1988. Computer programs for calculating total from specified free or free from specified total ionic concentrations in aqueous solutions containing multiple metals and ligands. *Methods Enzymol.* 157:378–417.

Ferris, C.D., R.L. Huganir, and S.H. Snyder. 1990. Calcium flux mediated by purified inositol 1,4,5-trisphosphate receptor in reconstituted lipid vesicles is allosterically regulated by adenine nucleotides. *Proc. Natl. Acad. Sci. USA*. 87:2147–2151.

Ferris, C.D., and S.H. Snyder. 1992. Inositol 1,4,5-trisphosphate-activated calcium channels. *Annu. Rev. Physiol.* 54:469–488.

Finch, E.A., T.J. Turner, and S.M. Goldin. 1991. Calcium as a coagonist of inositol 1,4,5-trisphosphate-induced calcium release. *Science.* 252:443–446.

Furuichi, T., K. Kohda, A. Miyawaki, and K. Mikoshiba. 1994. Intracellular channels. *Curr. Opin. Neurobiol.* 4:294–303.

Furuichi, T., S. Yoshikawa, A. Miyawaki, K. Wada, N. Maeda, and K. Mikoshiba. 1989. Primary structure and functional expression of the inositol 1,4,5-trisphosphate-binding protein P_{400}. *Nature.* 342: 32–38.

Harlow, E., and D. Lane. 1988. Antibodies: A Laboratory Manual. Cold Spring Harbor Laboratory Press, Cold Spring Harbor, NY. 78–81.

Iino, M. 1990. Biphasic Ca^{2+} dependence of inositol 1,4,5-trisphosphate-induced Ca release in smooth muscle cells of the guinea pig *taenia caeci*. *J. Gen. Physiol.* 95:1103–1122.

Iino, M. 1991. Effects of adenine nucleotides on inositol 1,4,5-trisphosphate-induced calcium release in vascular smooth muscle cells. *J. Gen. Physiol.* 98:681–698.

Islam, M.O., Y. Yoshida, T. Koga, M. Kojima, K. Kangawa, and S. Imai. 1996. Isolation and characterization of vascular smooth muscle inositol 1,4,5-trisphosphate receptor. *Biochem. J.* 316:295–302.

Kozak, M. 1987. An analysis of 5′-noncoding sequences from 699 vertebrate messenger RNAs. *Nucleic Acids Res.* 15:8125–8132.

Maeda, N., T. Kawasaki, S. Nakade, N. Yokota, T. Taguchi, M. Kasai, and K. Mikoshiba. 1991. Structural and functional characterization of inositol 1,4,5-trisphosphate receptor channel from mouse cerebellum. *J. Biol. Chem.* 266:1109–1116.

Mignery, G., T.C. Südhof, K. Takei, and P. De Camilli. 1989. Putative receptor for inositol 1,4,5-trisphosphate similar to ryanodine receptor. *Nature.* 342:192–195.

Mignery, G.A., C.L. Newton, B.T. Archer, and T.C. Südhof. 1990. Structure and expression of the rat inositol 1,4,5-trisphosphate receptor. *J. Biol. Chem.* 265:12679–12685.

Miyawaki, A., T. Furuichi, N. Maeda, and K. Mikoshiba. 1990. Expressed cerebellar-type inositol 1,4,5-trisphosphate receptor, P400, has calcium release activity in a fibroblast L-cell line. *Neuron.* 5:11–18.

Nakagawa, T., H. Okano, T. Furuichi, J. Aruga, and K. Mikoshiba. 1991*a*. The subtypes of the mouse inositol 1,4,5-trisphosphate receptor are expressed in a tissue-specific and developmentally specific manner. *Proc. Natl. Acad. Sci. USA*. 88:6244–6248.

Nakagawa, T., C. Shiota, H. Okano, and K. Mikoshiba. 1991*b*. Differential localization of alternative spliced transcripts encoding inositol 1,4,5-trisphosphate receptors in mouse cerebellum and hippocampus—in situ hybridization study. *J. Neurochem.* 57:1807–1810.

Supattapone, S., P.F. Worley, J.M. Baraban, and S.H. Snyder. 1988. Solubilization, purification, and characterization of an inositol trisphosphate receptor. *J. Biol. Chem.* 263:1530–1534.

Takei, K., G.A. Mignery, E. Mugnaini, T.C. Südhof, and P. De Camilli. 1994. Inositol 1,4,5-trisphosphate receptor causes formation of ER cisternal stacks in transfected fibroblasts and in cerebellar Purkinje cells. *Neuron.* 12:327–342.

Taylor, C.W., and A. Richardson. 1991. Structure and function of inositol trisphosphate receptors. *Pharmacol. Ther.* 51:97–137.

Worley, P.F., J.M. Baraban, S. Supattapone, V. Wilson, and S.H. Snyder. 1987. Characterization of inositol trisphosphate receptor binding in brain. *J. Biol. Chem.* 262:12132–12136.

Yamada, M., A. Miyawaki, K. Saito, T. Nakajima, M. Yamamoto-Hino, Y. Ryo, T. Furuichi, and K. Mikoshiba. 1995. The calmodulin-binding domain in the mouse type 1 inositol 1,4,5-trisphosphate receptor. *Biochem. J.* 308:83–88.